

# Exogenous High-Mobility Group Box 1 Protein Induces Myocardial Regeneration After Infarction via Enhanced Cardiac C-Kit<sup>+</sup> Cell Proliferation and Differentiation

Federica Limana\*, Antonia Germani\*, Antonella Zacheo, Jan Kajstura, Anna Di Carlo, Giovanna Borsellino, Omar Leoni, Roberta Palumbo, Luca Battistini, Raffaella Rastaldo, Susanne Müller, Giulio Pompilio, Piero Anversa, Marco E. Bianchi, Maurizio C. Capogrossi

**Abstract**—High-mobility group box 1 protein (HMGB1) is a chromatin protein that is released by inflammatory and necrotic cells. Extracellular HMGB1 signals tissue damage, stimulates the secretion of proinflammatory cytokines and chemokines, and modulates stem cell function. The present study examined exogenous HMGB1 effect on mouse left-ventricular function and myocyte regeneration after infarction. Myocardial infarction was induced in C57BL/6 mice by permanent coronary artery ligation. After 4 hours animals were reoperated and 200 ng of purified HMGB1 was administered in the peri-infarcted left ventricle. This intervention resulted in the formation of new myocytes within the infarcted portion of the wall. The regenerative process involved the proliferation and differentiation of endogenous cardiac c-kit<sup>+</sup> progenitor cells. Circulating c-kit<sup>+</sup> cells did not significantly contribute to HMGB1-mediated cardiac regeneration. Echocardiographic and hemodynamic parameters at 1, 2, and 4 weeks demonstrated a significant recovery of cardiac performance in HMGB1-treated mice. These effects were not observed in infarcted hearts treated either with the unrelated protein glutathione *S*-transferase or a truncated form of HMGB1. Thus, HMGB1 appears to be a potent inducer of myocardial regeneration following myocardial infarction. (*Circ Res.* 2005;97:0-0.)

**Key Words:** myocardial infarction ■ regeneration ■ stem cells ■ cytokines

Myocardial infarction (MI) is an irreversible injury where sudden interruption of blood flow caused by the occlusion of a coronary artery leads to cardiac myocyte death, tissue loss, and scar formation. Because the self-renewal capacity of adult cardiomyocytes is limited, the development of strategies to regenerate damaged myocardium and improve heart function represents a major challenge. A variety of bone marrow cell populations have been grafted into the damaged heart to improve its function and prevent remodeling and the progression to heart failure. Successful animal studies with bone marrow-derived cells led to clinical experimentation. However, the benefits observed in these pioneer trials are limited,<sup>1</sup> and there is a need to identify more effective strategies to induce cardiac regeneration if cell therapy of heart disease is to find a place in clinical practice. The identification of a stem cell population resident in the heart which supports myocardial regeneration has opened new opportunities for myocardial repair.<sup>2-6</sup> It may be possible to

explant resident cardiac stem cells from the heart, induce them to proliferate and differentiate *ex vivo*, and subsequently graft them into damaged heart. Alternatively, these cells may also be induced to proliferate, migrate, and differentiate after growth factor delivery in the infarcted heart,<sup>7</sup> without *ex vivo* manipulation.

High-mobility group box 1 protein (HMGB1) is a multifunctional protein which has both nuclear and extracellular functions. This protein is essential for survival because HMGB1-deficient mice die of hypoglycemia within 24 hours after birth.<sup>8</sup> HMGB1 was originally identified as a nonhistone DNA-binding nuclear protein; it binds DNA in a sequence-independent manner and modifies DNA structure to facilitate transcription, replication, and repair.<sup>9</sup> However, the intracellular localization of HMGB1 is not restricted to the nucleus, and in some cells this protein is also found in the cytoplasm.<sup>10</sup> The discovery that the sequence of HMGB1 is identical to that of heparin-binding protein amphoterin clearly attributed

Original received March 10, 2005; revision received April 20, 2005; resubmission received August 8, 2005; revised resubmission received August 29, 2005; accepted September 6, 2005.

From the Laboratorio di Patologia Vascolare, Istituto Dermopatico dell'Immacolata, Istituto di Ricovero e Cura a Carattere Scientifico (F.L., A.Z., O.L., M.C.C.), Rome, Italy; Laboratorio di Biologia Vascolare e Terapia Genica, Centro Cardiologico Fondazione Monzino, Istituto di Ricovero e Cura a Carattere Scientifico (A.G., A.di C., G.P.), Milan, Italy; Fondazione Santa Lucia (G.B., L.B.), Rome, Italy; Department of Molecular Biology and Functional Genomics, San Raffaele Research Institute (R.P., S.M.), Milan, Italy; Department of Medicine, New York Medical College (J.K., R.R., P.A.), Valhalla, New York; San Raffaele University (M.E.B.), Milan, Italy.

\*Both authors contributed equally to this work.

Correspondence to Maurizio C. Capogrossi, Laboratorio di Patologia Vascolare, Istituto Dermopatico dell'Immacolata-IDI, Via dei Monti di Creta 104, 00167 Rome, Italy. E-mail capogrossi@idi.it

© 2005 American Heart Association, Inc.

*Circulation Research* is available at <http://circres.ahajournals.org>

DOI: 10.1161/01.RES.0000186276.06104.04

to HMGB1 an extracellular role. In transformed cells, HMGB1 is located in the leading edges of migrating cells, and it is secreted (by an unknown mechanism) into the extracellular space, suggesting a key role in regulating cell migration and metastasis.<sup>11–13</sup> Recently, a novel role for HMGB1 as a cytokine was identified. HMGB1 is a potent mediator of inflammation; it is secreted by activated macrophages in response to proinflammatory cytokines<sup>14–16</sup> and released passively from necrotic cells.<sup>17</sup> Moreover, when added to endothelial cells, HMGB1 elicits proinflammatory responses by increasing the expression of vascular adhesion molecules as well as secretion of cytokines (tumor necrosis factor- $\alpha$ ) and chemokines (interleukin [IL]-8 and monocyte chemoattractant protein-1).<sup>18</sup>

Several lines of evidence demonstrated that the effects of the extracellular HMGB1 are mediated, at least in part, by its binding to the receptor for advanced glycation end products (RAGE), a multiligand receptor of the immunoglobulin superfamily.<sup>19,20</sup> Interaction of HMGB1 with RAGE induces neurite outgrowth in the developing nervous system as well as neuronal differentiation of embryonic stem cells<sup>21</sup> and rat smooth-muscle cell chemotaxis.<sup>22</sup> Furthermore, it has been reported that HMGB1 is a strong chemoattractant and a pro-proliferative molecule for vessel-associated stem cells (mesoangioblasts).<sup>23</sup> The ability of HMGB1 to act as a signal of tissue damage and to promote proliferation, migration, and differentiation of several stem cell types prompted us to evaluate whether exogenous HMGB1 could elicit myocardial regeneration after infarction by modulating cardiac stem cell function.

## Materials and Methods

### HMGB1 Production

Expression and purification of glutathione *S*-transferase (GST) and HMGB1 proteins as well as its truncated form (boxA)<sup>22</sup> were performed as previously described.<sup>24</sup> Endotoxins were removed by passage through Detoxy-Gel columns (Pierce Biotechnology Inc).

### Animals, Surgical Procedures, and Proteins Injection

MI was induced in C57BL/6 mice as previously described.<sup>25</sup> In short, in mice under anesthesia (100 mg/kg ketamine and 1 mg/kg acepromazine) and mechanically ventilated, thoracotomy via the third left-intercostal space was performed and the left coronary artery was ligated. The chest was closed and the mice were allowed to recover. Sham-operated mice were treated similarly, except that the ligature around the coronary artery was not tied. After 4 hours animals were reoperated, and 200 ng of purified HMGB1 in 10  $\mu$ L PBS solution containing rhodamine spheres was injected through a 32-gauge needle. Four injections (2.5  $\mu$ L per injection) were made in the ventricular wall bordering the viable myocardium. Successful injection was indicated by the presence of rhodamine in the site of injection. Control infarcted mice were injected with 200 ng either of GST, an unrelated protein, or boxA. Animals were killed 1, 2, and 4 weeks after surgery. All experimental procedures complied with the Guidelines of the Italian National Institutes of Health, with the Guide for the Care and Use of Laboratory Animals (Institute of Laboratory Animal Resources, National Academy of Sciences), and were approved by the Institutional Animal Care and Use Committee.

### Immunohistochemical Analysis

Hearts were arrested in diastole with CdCl<sub>2</sub>, perfused retrogradely with 10% (vol/vol) formalin, embedded in paraffin, and sectioned

(3  $\mu$ m thickness). The following antibodies were used to identify cardiac stem cells and to assess cardiac differentiation: mouse monoclonal c-kit antibody (DakoCytomation, Carpinteria, Calif), rabbit polyclonal connexin 43 antibody (Sigma, St. Louis, Mo), mouse monoclonal anti- $\alpha$ -sarcomeric actin (clone 5C5; Sigma), rabbit polyclonal anti-MEF2C (C-21; Santa Cruz Biotechnology, Santa Cruz, Calif). Ki67 was detected with mouse polyclonal antibody (clone NCL; Novocastra Laboratories, UK). Fluorescein isothiocyanate (FITC)-conjugated goat anti-rabbit and tetramethylrhodamine-5-(and 6)-isothiocyanate-conjugated goat anti-mouse (Sigma) were used as secondary antibodies.

HMGB1 in heart tissue was detected using rabbit polyclonal antibody (1  $\mu$ g/mL; BD Pharmingen, San Diego, Calif) after incubation with biotinylated secondary antibodies (7.5  $\mu$ g/mL; Vector Laboratories, Peterborough, UK), and with avidin-biotinylated peroxidase complex (ABC Elite Kit; Vector Laboratories). The staining was visualized by treatment for 10 minutes in a 0.05% solution of 3-diaminobenzidine and 0.01% H<sub>2</sub>O<sub>2</sub> in PBS. Sections were counterstained with hematoxylin to identify nuclei. Control reactions included the omission of the primary antibody, which was substituted by nonimmune goat serum.

### Evaluation of Myocardial Function

Echocardiography was performed in conscious mice with a Sequoia 256c equipped with a 13-MHz linear transducer. Two-dimensional images and M-mode tracings were recorded from the parasternal short axis view at the level of papillary muscle. From M-mode tracings, anatomical parameters in diastole and systole were obtained.<sup>26</sup> For hemodynamic studies, mice were anesthetized with chloral hydrate (400 mg/kg body weight), and the right carotid artery was cannulated with a microtip pressure transducer (Millar 1.4F).

### Cardiac Anatomy and Infarct Size

After hemodynamic measurements, the abdominal aorta was cannulated, the heart was arrested in diastole, and the left ventricular (LV) chamber was fixed at a pressure equal to the *in vivo* measured end-diastolic pressure. The LV intracavitary axis was measured, and three transverse slices from the base, mid-region, and apex were embedded in paraffin. The midsection was used to measure LV thickness, chamber diameter, and volume as described.<sup>6,25,27</sup> The chamber volume was calculated using the minimal and maximal luminal diameters at middle-region with the longitudinal axis. Diastolic wall stress was determined from the wall thickness, chamber radius, and LV end-diastolic pressure (LVEDP). In each LV cross section, the infarct length was calculated by measuring the endocardial and epicardial surface length delimiting the infarcted region and the total LV. Infarct size (in percent) was calculated as infarct length divided by the total LV circumference.<sup>28</sup>

### RT-PCR

RNA was extracted with TRIzol (Invitrogen). Preamplication system was used to reverse-transcribe total RNA (1  $\mu$ g) into complementary DNA according to manufacturer's instructions (Invitrogen). An aliquot (2  $\mu$ L) of the reverse transcription reaction was subjected to 39 polymerase chain reaction cycles: 1 minute at 94°C, 1 minute at 58°C, and 1 minute at 72°C, in the presence of 50 pmol of each primer, 1.5 mmol/L MgCl<sub>2</sub>, 200 mmol/L dATP, dCTP, dGTP, and dTTP, and 2.5 U of Amplitaq polymerase (Invitrogen). Sequences of the primers were: Nkx2.5 5'-GAG TGG AGC TGG ACA AAG CC-3' and 5'-TAG CGA CGG TTC TGG AAC CA-3'; c-kit 5'-CTG ACC TAC GGC GTG CAG TG-3' and 5'-GTT CTG CTG GTA GTG GTC GG-3'; actin 5'-CACCTTCTACAATGAGCT-3' and 5'-GAAGGTAGTCTGTCAGGTC-3'. The polymerase chain reaction products were electrophoresed on a 1.5% agarose gel containing 0.5  $\mu$ g/mL ethidium bromide.

### Cardiac C-Kit<sup>+</sup> Cell Isolation and Culture

Cardiac c-kit<sup>+</sup> cells were isolated from 2- to 3-month-old C57BL/6J male mice as previously described.<sup>4</sup> Hearts were explanted and perfused with a collagenase solution (280 U/mL; Worthington,

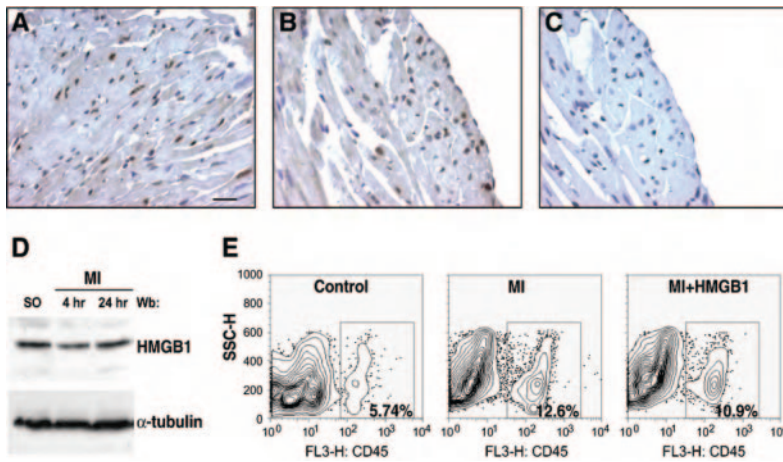


**Figure 1.** HMGB1 is expressed in the heart. Immunohistochemical analysis of HMGB1 expression in (A) noninfarcted and (B) infarcted heart 24 hours after infarction. C, Control immunostaining was performed by omitting the primary antibody. Bar=25  $\mu$ m. D, Western blot analysis of protein extracts (100  $\mu$ g) from ventricles of sham-operated (SO) and infarcted hearts (MI) at 4 and 24 hours after coronary artery ligation. Proteins were resolved by SDS-PAGE, transferred to nitrocellulose filter, and probed with HMGB1 antibody. The same filter was probed with anti- $\alpha$ -tubulin mAb to show equal protein concentration. This result was obtained from 3 independent experiments. E, FACS analysis to detect CD45<sup>+</sup> cells in control and infarcted hearts, untreated (MI) and HMGB1-treated (MI+HMGB1), 24 hours after infarction. The number of CD45<sup>+</sup> cells increased after infarction, and HMGB1 did not modify their number. The experiments reported in this figure were repeated twice with similar results.

Lakewood, N.J.) to dissociate cardiac cells. After removal of myocytes by centrifugation, cell suspension was incubated with a mouse phycoerythrin-conjugated c-kit antibody (BD Pharmingen; San Diego, Calif) and cells were sorted on a MoFlo triple-laser flow cytometer and SUMMIT software (Cytomation). Cells were also characterized for expression of CD11b, Gr1, B220, and CD45.

Isolated c-kit<sup>+</sup> cells were fixed in PBS with 4% paraformaldehyde and permeabilized in PBS with 0.1% Triton X-100. Coverslips were rinsed and blocked 10 minutes in PBS with 0.2% BSA before incubation with antibodies. Fixed cells were incubated with primary antibodies: goat polyclonal anti-Nkx2.5 (N19, Santa Cruz Biotechnology), rabbit polyclonal anti-GATA4 (H112, Santa Cruz Biotechnology), and goat polyclonal anti-RAGE (Abcam, Cambridge, UK). Then, the fixed cells were incubated with antibodies coupled either with FITC or tetramethylrhodamine-5-(and 6)-isothiocyanate. The coverglasses were mounted and analyzed with a Zeiss microscope equipped for epifluorescence.

For in vitro proliferation assay, c-kit<sup>+</sup> cells were isolated and cultured in F12K medium supplemented with 20% fetal bovine serum (FCS; Euroclone Inc, Milan, Italy), 20 mmol/L Glutamine, 100 U/mL Penicillin, and 100 mg/mL Streptomycin (Growth medium-GM; Gibco BRL, Paisley, UK). After 24 hours, the medium was replaced with serum-free F12K for 16 hours. Then, cells were grown with medium containing BrdU (10  $\mu$ mol/L) either in absence or presence of 100 ng/mL of HMGB1 for 24 hours.

### Chemotaxis Assay

Chemotaxis was performed in 48-microwell chemotaxis chambers (Neuroprobe) using 3- $\mu$ m pore-size polycarbonate filters (Costar Scientific Corporation) coated with murine collagen type IV (Becton-Dickinson, Bedford, Mass).

The lower compartment of each chamber was filled with 28  $\mu$ L F12K with 0.1% BSA. Each well of the upper compartment contained cardiac c-kit cells ( $4 \times 10^5$  cells/mL) in 50  $\mu$ L F12K either with 0.1% BSA (negative control) or 100 ng/mL HMGB1. Each point was run in triplicate. After 6 to 8 hours incubation at 37°C in a 5% CO<sub>2</sub> humidified atmosphere, the chemotaxis assay was stopped, and cells on the filter were fixed and stained using Diff Quik (Dade AG). Cells in 5 random fields on the lower face of the filter were counted at 40 $\times$  magnification, and migration index was calculated by dividing the number of migrated cells in the presence of chemoattractants by the cells migrated in response to DMEM with 0.1% BSA.

### Peripheral Blood C-Kit<sup>+</sup> Cells and Hematopoietic Colony Assay

Peripheral blood mononucleated cells (PBMCs) were obtained by Ficoll gradient separation of blood. To detect c-kit<sup>+</sup> cells, PBMCs were incubated for 30 minutes at 4°C in PBS containing 5% FCS with phycoerythrin-conjugated anti-c-kit monoclonal antibody, and then analyzed by flow cytometry.

To evaluate bone marrow stem cell mobilization into the systemic circulation,  $4 \times 10^4$  PBMCs were plated on methylcellulose medium containing IL-6, IL-3, and Stem Cell Factor. After 14 days the total number of colonies was counted.

### Bone Marrow C-Kit Cells Delivery in Mice

Bone marrow c-kit<sup>+</sup> cells were isolated as previously described.<sup>28</sup> Purified c-kit<sup>+</sup> cells were cultured in a medium containing 5-bromo-2'-deoxy-uridine (BrdU, 10  $\mu$ M) for 16 hours. After this time, 90% of cells incorporated BrdU. Cells were then injected in the tail vein of mice ( $5 \times 10^5$  cells per mouse) immediately after coronary artery ligation. HMGB1 was injected in the myocardium as described above. Animals were euthanized 1 week later and hearts processed for immunohistochemical analysis. Paraffin heart sections were stained with monoclonal anti-BrdU antibody (Roche, Indianapolis, Ind) followed by FITC rabbit anti-mouse antibody.

### Western Blot Analysis

Proteins from heart tissue (ventricles) were homogenized and extracted with RIPA buffer (10 mmol/L Tris-HCl pH 7.4, 150 mmol/L NaCl, 1% NP40, 1% Deoxycolic acid, 0.1% SDS, and 10% Glycerol) containing protease and phosphatase inhibitors (2 mmol/L phenylmethylsulfonyl fluoride, 100 U/mL of aprotinin, 10  $\mu$ g/mL of leupeptin and pepstatin, 10 mmol/L sodium fluoride, 20 mmol/L sodium vanadate). Equal amounts of total cellular proteins (100  $\mu$ g/lane) were resolved by SDS-polyacrylamide gel electrophoresis and transferred to nitrocellulose membrane (Amersham Pharmacia Biotech). Membranes were probed with HMGB1 rabbit polyclonal antibody (1  $\mu$ g/mL BD Pharmingen), and  $\alpha$ -tubulin monoclonal antibody (0.1  $\mu$ g/mL, Oncogene Science Inc., Cambridge, Mass), followed by horseradish peroxidase-coupled secondary antibodies, and developed by a chemiluminescence-based detection system (ECL, Amersham Pharmacia Biotech).

### Two-Photon Microscopy

C-kit<sup>+</sup> cells were labeled by injection of a retroviral vector expressing enhanced green fluorescence protein (EGFP) 3 days before coronary occlusion. HMGB1 was administered after MI, and hearts were examined 20 hours after infarction. The heart was excised, perfused retrogradely through the aorta with Tyrode solution containing 30 mmol/L KCl, and placed in a bath mounted on top of the microscope stage of a two-photon microscope (Bio-Rad Radiance 2100MP). The heart was continuously perfused and superfused at 37°C with oxygenated Tyrode solution containing rhodamine-labeled dextran. The two-photon microscope was positioned to view the LV free wall. EGFP and rhodamine were excited at 960 and 840 nm, respectively, with mode-locked Ti:Sapphire femtosecond laser (Tsunami, Spectra-Physics). Four-dimensional image stacks were acquired at emission wavelengths of 515 and 600 nm, respectively. The region between the atrial and ventricular groove and the

middle-region of the infarcted heart was continuously monitored for 4 hours.

### Volume of Newly Formed Myocytes

The volume of newly formed myocytes were calculated as previously reported.<sup>25,27</sup>

### Data Collections and Statistics

Immunohistochemic, hemodynamic, and echocardiographic analyses were examined blindly. Results are presented as mean±standard deviation. Statistical significance between 2 measurements was evaluated by unpaired Student *t* test, and multiple comparisons were performed by Bonferroni method. A probability value of  $P<0.05$  was considered significant.

## Results

### HMGB1 Induces Myocardial Cell Regeneration in the Infarcted Heart

HMGB1 is expressed in the heart tissue where it localizes in the nucleus of cardiomyocytes. At 24 hours after infarction, neither HMGB1 intracellular localization (Figure 1A through 1C) nor HMGB1 protein levels (Figure 1D) were modified. Recombinant HMGB1 was injected into the peri-infarcted LV myocardium 4 hours after infarction, before the occurrence of necrosis, as previously demonstrated by the lack of staining with hairpin probe.<sup>29</sup> Therefore, at this time point, intracellular HMGB1 had not been released into the extracellular space by necrotic cells. Control hearts were treated either with the unrelated protein GST or with boxA.<sup>22</sup> HMGB1 treatment did not further increase inflammatory cell recruitment compared with untreated infarcted hearts. Indeed, the percentage of cells expressing the hematopoietic marker CD45<sup>+</sup> was similar between untreated and HMGB1-treated hearts 24 hours after infarction (Figure 1E).

One week after infarction, the injured area in the HMGB1-treated ventricle was partially reconstituted by a population of myocardial cells (Figure 2A). These cells were smaller, spatially less organized than normal adult myocardial cells, and were detected in 9 of 13 HMGB1-injected hearts. In contrast, control infarcted ventricles were characterized by scar tissue with few sparse myocardial cells (Figure 2B). At 2 and 4 weeks after infarction, regenerating bands were detected in 10 of 13 and 10 of 12 hearts injected with HMGB1, respectively.

Newly formed cells detected in the infarcted ventricle expressed  $\alpha$ -sarcomeric actin, a specific marker of cardiac differentiation (Figure 2A and 2C). These cells occupied most of the damaged area extending from the border zone throughout the infarcted LV free wall (Figure 2A). In contrast, expression of  $\alpha$ -sarcomeric actin was restricted only to the surviving myocytes in GST- (Figure 2D) and boxA-treated hearts (data not shown).  $\alpha$ -sarcomeric actin-expressing cells were also positive for MEF2C, a transcription factor that identifies mature cardiomyocytes and that is involved in the activation of several cardiac structural genes (Figure 2E). To evaluate whether these cells were cycling, the expression of Ki67 (a protein present in G1, S, G2, and early mitosis) was examined. In HMGB1-treated hearts, Ki67 was expressed in  $\alpha$ -sarcomeric actin-positive cells (Figure 2F) suggesting that the newly formed cells were derived from proliferating cells.

We also assessed the expression of connexin 43 (Cx43), a gap-junctional molecule responsible for electrical coupling between cardiomyocytes. In noninfarcted heart, Cx43 was abundantly distributed at the junctions between cardiomyocytes (Figure 3A). In HMGB1-treated hearts at 1 week after coronary artery occlusion, Cx43 was detected as a punctuate staining at the surface of some newly formed cardiomyocytes (Figure 3B), and its expression strongly increased 2 weeks after infarction (Figure 3C), demonstrating that the new myocardial cells were acquiring functional competence. Newly formed cells in HMGB1-injected heart were signifi-

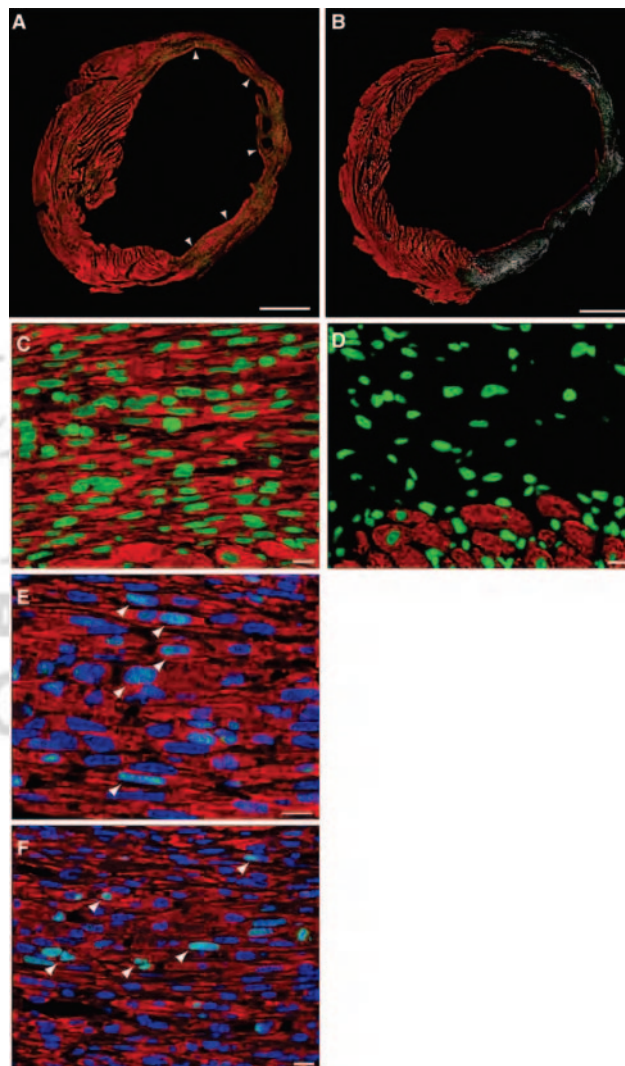


**Figure 2.** HMGB1 induces newly formed  $\alpha$ -sarcomeric expressing cells in the infarcted heart. A and B, Low-power view of  $\alpha$ -sarcomeric actin immunostaining (red fluorescence) of infarcted mouse heart, treated with HMGB1 (A) and GST (B) and euthanized 1 week later. Arrowheads indicate a band of regenerated myocardium. GST-treated heart was also stained for collagen I and III (white fluorescence) to evidence scar tissue formation and a thin endocardial layer of  $\alpha$ -sarcomeric actin positive cells. Bar=1 mm.  $\alpha$ -sarcomeric actin immunostaining of infarcted HMGB1 (n=9) (C) and GST (n=25) treated hearts (D). Bar=10  $\mu$ m. Red fluorescence,  $\alpha$ -sarcomeric actin; green false color, Propidium iodide (PI). E, Newly formed cells positive for  $\alpha$ -sarcomeric actin (red fluorescence) expressed MEF2-C and (F) Ki67 as indicated by the arrows (light blue fluorescence). Bar=10  $\mu$ m. Blue false color, PI in nuclei.

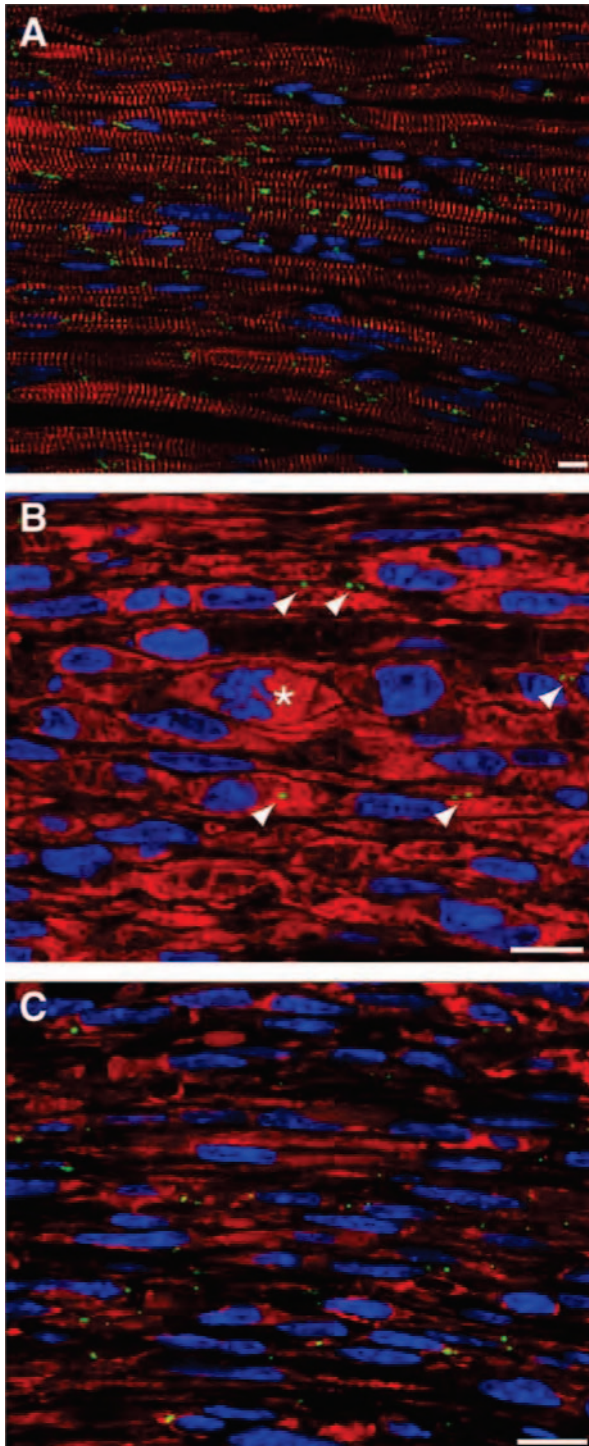


**Figure 3.** Newly formed myocytes in the infarcted area express connexin 43. A, Connexin 43 is detected as punctuate staining (green fluorescence) in the gap-junctional regions between cardiomyocytes in noninfarcted hearts. At 1 week after infarction, connexin 43 was apparent (B) and its expression increased at 2 weeks (n=4 for each group) (C). \* indicates cell in mitosis. Bar=10  $\mu\text{m}$ . Red fluorescence,  $\alpha$ -sarcomeric actin; blue false color, PI in nuclei.

cantly smaller than mature cardiomyocyte. They had a volume of  $411 \pm 136 \mu\text{m}^3$  with a wide size distribution (43.2% between 70 and 300  $\mu\text{m}^3$ , 37.9% between 300 and 600  $\mu\text{m}^3$ , 18.9% >600  $\mu\text{m}^3$ ), which is markedly lower than adult

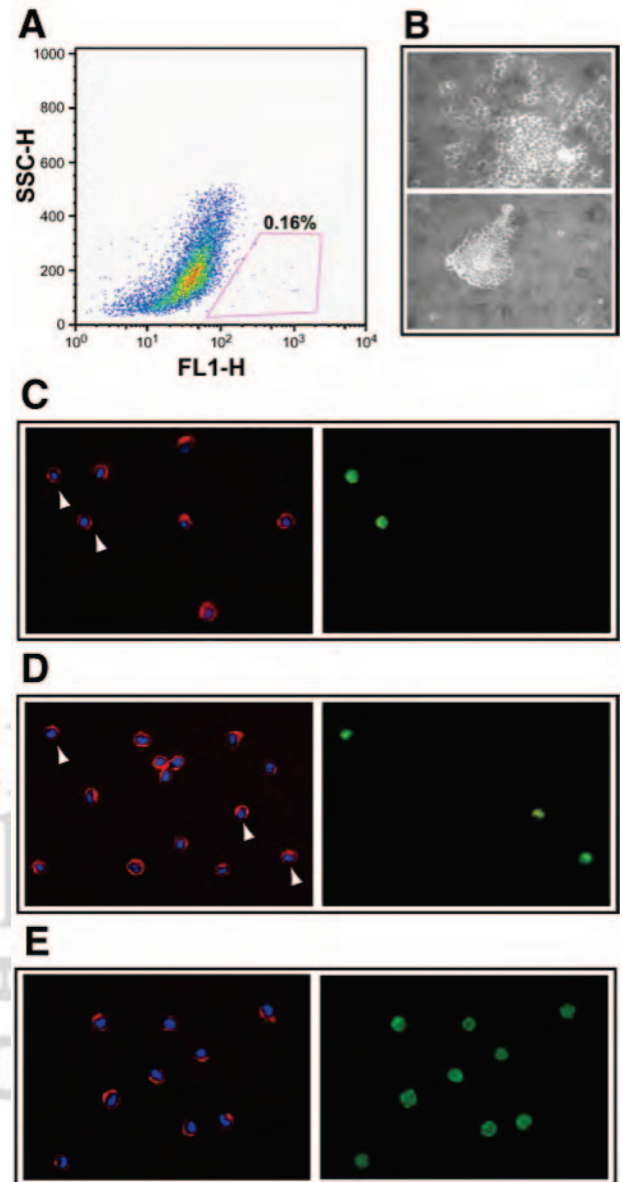


**Figure 4.** In vitro analysis of cardiac c-kit<sup>+</sup> cells. A, Flow cytometry analysis of c-kit<sup>+</sup> cells isolated from the whole control heart. B, FACS-sorted cardiac c-kit<sup>+</sup> cells formed hematopoietic colonies in Methocult M3434. C through E, Freshly isolated c-kit<sup>+</sup> cells from control heart (red fluorescence in left panels) expressed Nkx2.5 (C), GATA-4 (D), and RAGE (E) (all in green fluorescence in right panels). Blue false color, PI in nuclei.

mouse myocyte volume (ie,  $\approx 13\,000 \mu\text{m}^3$ ).<sup>30</sup> This finding supports the evidence that these cells were newly formed myocytes and were not derived from myocytes which had survived in the infarcted region. Taken together, these data demonstrate that the injection of exogenous HMGB1 induces cardiomyocyte formation in the infarcted heart.

### HMGB1 Induces Cardiac Stem Cell Proliferation and Differentiation

To assess the origin of the newly formed myocardial cells in HMGB1-injected hearts, cardiac stem cells expressing c-kit antigen (c-kit<sup>+</sup>) were evaluated. Prior studies have shown that these cells are involved in myocardial regeneration.<sup>4-6,31</sup>

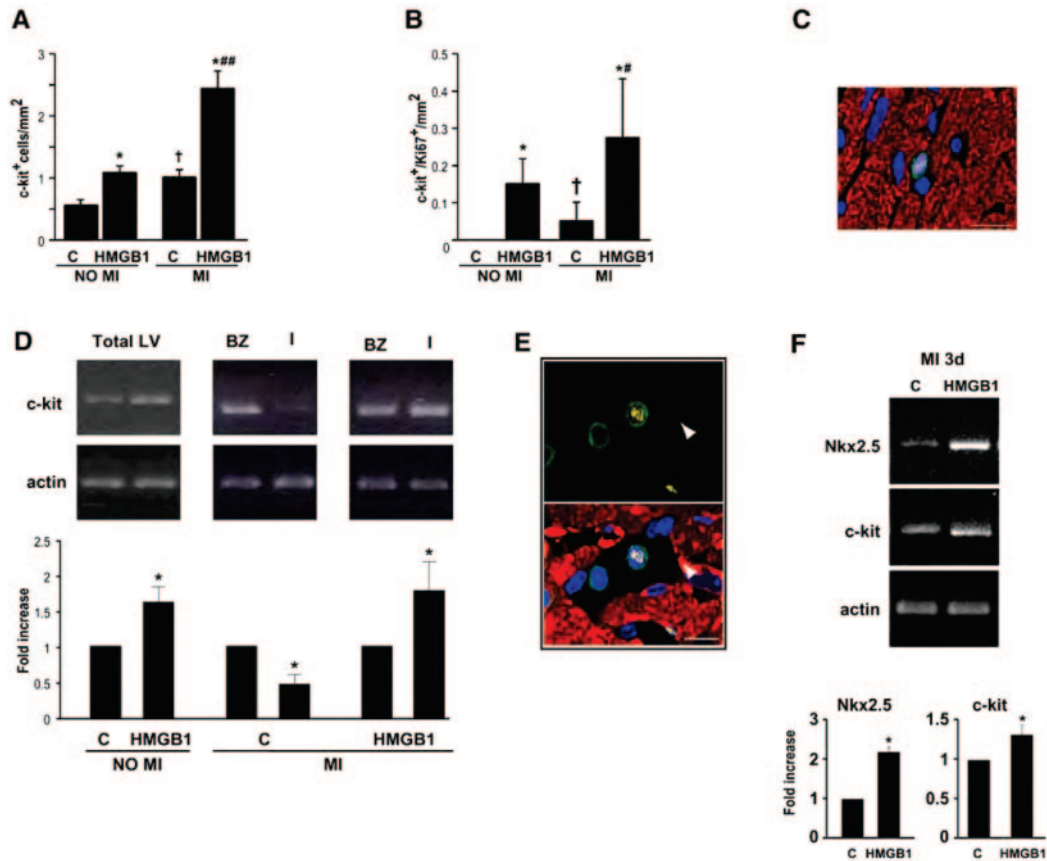


**Figure 5.** HMGB1 induced in vivo proliferation and differentiation of c-kit<sup>+</sup> cells. Effect of HMGB1 on c-kit<sup>+</sup> cell proliferation. A and B, Bar graph of the (A) mean c-kit<sup>+</sup> and (B) c-kit<sup>+</sup>/Ki67 double positive cells in noninfarcted (NO MI) and infarcted hearts (MI), treated either with HMGB1 or GST (C), analyzed 24 hours after coronary artery ligation and HMGB1 injection (n=6 for each group; \*P<0.001 vs C; †P<0.001 vs C NO MI; ##P<0.05 and ###P<0.001 vs HMGB1, NO MI). C, Representative picture showing c-kit (green) and Ki67 (white) positive cell (arrow) in heart tissue 24 hours after infarction and HMGB1 treatment. D, Semiquantitative RT-PCR analysis of c-kit expression in total LV (Total LV) of noninfarcted hearts as well as in the border zone (BZ) and infarcted tissue (I) after treatment either with GST (C) or HMGB1. Lower panel, Average results of densitometric analysis of RT-PCR shown in (D) (n=3, P<0.05). E, Upper panel, c-kit (green) and MEF2C (yellow) expression in HMGB1-treated heart, 3 days after coronary artery ligation. Lower panel,  $\alpha$ -sarcomeric actin (red) immunostaining of the same section shown in the upper panel; c-kit (green), MEF2C (white). The arrow indicates c-kit/MEF2C double positive cell. Bar=10  $\mu$ m. Blue, PI in nuclei. F, Semiquantitative RT-PCR analysis of Nkx2.5 and c-kit expression in total heart tissue, treated either with HMGB1 or GST (C) 3 days after coronary artery ligation. Lower panel, Average results of densitometric analysis of RT-PCR shown in G (n=3, P<0.05).

After separation from differentiated myocytes, c-kit<sup>+</sup> cells represented  $0.2 \pm 0.24\%$  of the mouse heart cells (Figure 4A); they were negative for markers of myeloid, lymphoid, and erythroid lineages (CD45, CD11b, Gr1, Ter119)<sup>4</sup> (data not shown), but displayed the capacity to form hematopoietic colonies when cultured in methylcellulose medium containing stem cell factor, IL-3, and IL-6 (Figure 4B). Occasionally, freshly isolated c-kit<sup>+</sup> cells from noninfarcted hearts expressed early markers of myocardial development, Nkx2.5 and GATA4<sup>4</sup> (Figure 4C and 4D). Interestingly, all cardiac c-kit<sup>+</sup> cells were positive for the HMGB1 receptor, RAGE (Figure 4E), in agreement with the concept that HMGB1 may modulate the functional properties of these cells. To address whether HMGB1 induced proliferation of cardiac c-kit<sup>+</sup> cells, hearts were injected with HMGB1 either in the absence or in the presence of infarction, and c-kit<sup>+</sup> cells were identified by immunostaining 24 hours later. c-kit<sup>+</sup> cells increased  $\approx 2$ -fold in the heart after infarction compared with GST-treated noninfarcted heart. HMGB1 treatment enhanced

c-kit<sup>+</sup> cell numbers both in noninfarcted and infarcted hearts (Figure 5A). Proliferating c-kit<sup>+</sup> cells, detected as c-kit/Ki67 double positive cells, were present in HMGB1-injected hearts, whereas no proliferating c-kit<sup>+</sup> cells were observed in hearts injected with the control protein GST (Figure 5B). After infarction c-kit<sup>+</sup> proliferating cells appeared in GST-treated hearts, and their numbers increased  $\approx 7$ -fold in response to HMGB1 treatment (Figure 5B and 5C). In agreement with these data, 24 hours after HMGB1 treatment, c-kit<sup>+</sup> expression increased in the left ventricle of noninfarcted HMGB1-treated heart as well as in the infarcted tissue from HMGB1-treated heart (Figure 5D and 5E). In contrast, HMGB1 had no effect in vitro on the proliferation of isolated cardiac c-kit<sup>+</sup> cells, as assessed as BrdU incorporation rate (data not shown). It is noteworthy that differentiating cells were detected only in infarcted HMGB1-treated hearts. At day 3 after infarction, cells coexpressing c-kit and MEF2C were detected in HMGB1-treated hearts cells (Figure 5F). At the same time, mRNA expression of both c-kit and Nkx2.5,

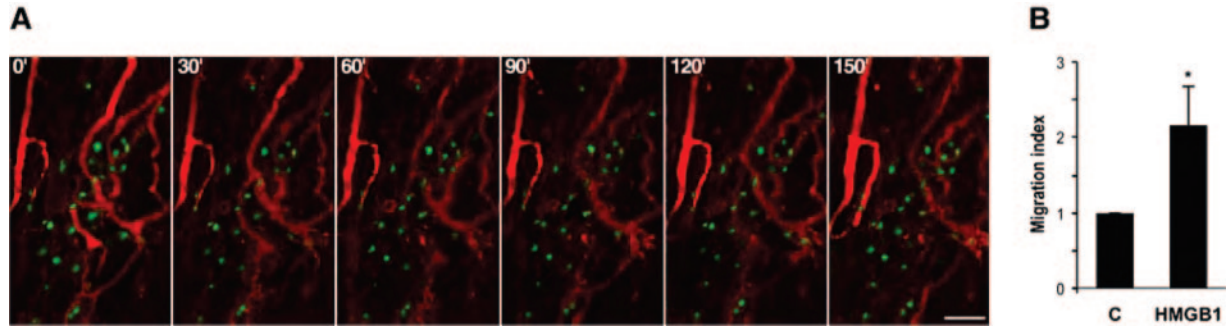


**Figure 6.** Effect of HMGB1 on c-kit<sup>+</sup> migration. A, Ex vivo monitoring of c-kit<sup>+</sup> cell migration. Cardiac progenitor cells were labeled by injecting an EGFP retroviral vector 3 days before coronary artery ligation. HMGB1 (200 ng/heart) was administered 4 hours after MI. Hearts were examined 20 hours later (n=8). Migration was followed by two-photon microscopy. Images were obtained every 30 minutes and show that there was no locomotion of EGFP expressing cells. Bar=50  $\mu$ m. B, In vitro migration of c-kit cells in response to HMGB1 (100 ng/mL). BSA (0.1%) was used as negative control (C). Data are expressed as the fold increase in the number of migrated cells relative to the number of migrated cells in the negative control (migration index) and are the means $\pm$ SD of at least 4 independent experiments performed in triplicate.

an early transcription factor of the cardiomyocyte lineage, increased in infarcted HMGB1-treated hearts (Figure 5G and 5H).

In additional experiments the chemotactic effect of HMGB1 on cardiac c-kit cells was examined both ex vivo by two-photon microscopy<sup>2-6</sup> and in vitro. In the two-photon microscopy experiments, the region between the atrial and ventricular groove and the middle-region of the infarcted heart was continuously monitored for 4 hours. In both heart regions, the EGFP-tagged cells remained in position without any apparent locomotion (Figure 6A). In contrast, in the in vitro assay performed with modified Boyden chambers, HMGB1 enhanced c-kit<sup>+</sup> cell chemotaxis. The migratory effect was  $\approx$ 2-fold higher compared with the negative control (Figure 6B).

Taken together, these data indicate that HMGB1 promotes c-kit<sup>+</sup> cell proliferation in vivo both in control and infarcted hearts. However, HMGB1 ability to induce stem cell differentiation toward the cardiomyocyte lineage was observed only in the infarcted heart. Although HMGB1 induced stem cell migration in vitro, under the ex vivo experimental conditions used in the present study, no migratory effect on cardiac cells was detected.

### Effect of HMGB1 on Bone Marrow–Derived Stem Cells

To address the contribution of bone marrow–derived stem cells in HMGB1-mediated cardiac tissue regeneration, it was examined whether HMGB1 induced stem cell mobilization from the bone marrow. Clonogenic assay on methylcellulose with PBMCs obtained from both GST and HMGB1-treated infarcted mice revealed no difference in the total number of colonies (Figure 7A). Moreover, FACS analysis showed that, whereas c-kit<sup>+</sup> cells in the peripheral blood increased after MI, HMGB1 treatment did not yield any significant change in the circulating c-kit<sup>+</sup> cells number either in presence or absence of infarction (Figure 7B).

To examine whether HMGB1 enhanced circulating c-kit<sup>+</sup> cell homing to the heart, BrdU-labeled bone marrow (BM) c-kit<sup>+</sup> cells were injected in the mouse tail vein immediately after MI followed by HMGB1 and GST treatment. As

evidenced by BrdU immunostaining 7 days later, BM-derived c-kit<sup>+</sup> cells were detected in the infarcted area as well as in survived myocardium (Figure 8A and 8B). Although there was an increase of BM-c-kit<sup>+</sup>/BrdU<sup>+</sup> cells in HMGB1 compared with GST-treated mice, this difference was not statistically significant (Figure 8B). Most importantly, regenerating newly formed  $\alpha$ -sarcomeric actin–expressing myocytes were BrdU<sup>–</sup> (Figure 8A). Taken together, these data suggest that newly formed cells in infarcted HMGB1-treated hearts are of cardiac origin rather than derived from the systemic circulation.

### HMGB1 Improves Cardiac Function

Functional studies were performed to determine whether myocardial regeneration was associated with an improvement in cardiac function. Echocardiographic and hemodynamic studies were performed 1, 2, and 4 weeks after infarction. In comparison with sham-operated mice, infarcted animals treated with control proteins (GST or boxA) exhibited evi-

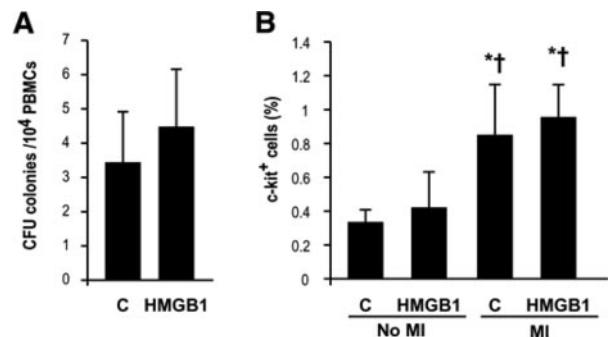


**Figure 7.** Effect of HMGB1 treatment on circulating stem cells. A, Bar graph indicating GM-CFU number obtained culturing PBMCs in Methocult M3434, after their isolation from 24-hour infarcted heart treated either with GST (C) or HMGB1. Data are expressed as means of 4 experiments  $\pm$ SE. B, Bar graph of flow cytometric measurements of c-kit<sup>+</sup> cell number in peripheral blood from noninfarcted (NO MI), infarcted (MI) hearts treated either with GST (C) or HMGB1. Analysis was performed by use of phycoerythrin-conjugated anti-c-kit antibody and is shown as percent of total PBMCs. Data are expressed as means of 6 experiments  $\pm$ SE; \* and †,  $P < 0.05$  vs noninfarcted C and HMGB1, respectively.

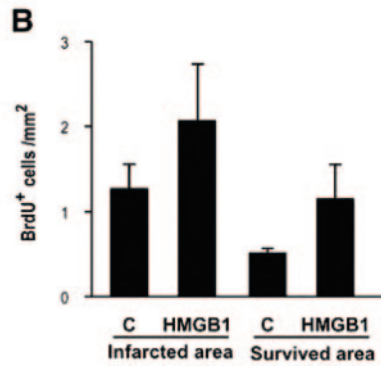
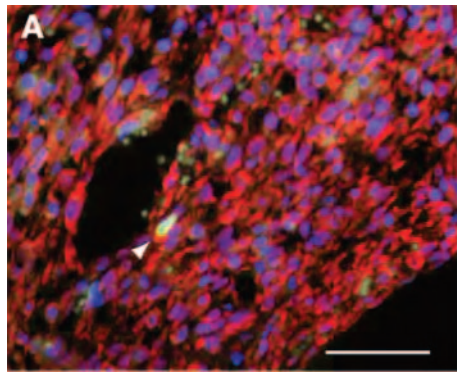


**Figure 8.** Contribution of BM-derived c-kit<sup>+</sup> cells in HMGB1-mediated cardiac tissue regeneration. A, Section of infarcted HMGB1-treated heart 7 days after coronary occlusion and BM-c-kit<sup>+</sup> injection. BM-c-kit<sup>+</sup>-derived cells were identified by BrdU immunostaining (green fluorescence). Arrow-head indicates a BrdU<sup>+</sup> cell. The same section was stained with  $\alpha$ -sarcomeric actin (red fluorescence) and Hoechst to evidence nuclei (blue color). Bar=50  $\mu$ m. B, Bar graph of the mean of circulating BM-derived c-kit<sup>+</sup> cells in the infarcted area and in the survived area of GST (C) and HMGB1 treated heart (n=3). The difference between C and HMGB1 groups was not statistically significant.

dence of cardiac failure (Figures 9 through 11). In mice treated with HMGB1, M-mode echocardiography demonstrated an enhanced contractile function at 1 week after infarction (Figure 9A through 9D). Ejection Fraction was 24%, 49%, and 62% higher in HMGB1-treated than in GST-treated mice at 1, 2, and 4 weeks after infarction, respectively (Figure 9E and Table). Hemodynamic measurements demonstrated an enhanced cardiac performance versus controls at all time points (Figure 10A through 10C). LVEDP was between 41% to 48% lower in HMGB1-treated versus GST-treated mice at 1, 2, and 4 weeks postinfarcted hearts; these values reached levels similar to those of sham-operated

mice (Figure 10A and Table). LV+dP/dT and -dP/dT in HMGB1-treated mice exhibited a 40% and 35% increase above control, respectively, at 4 weeks after infarction (Figure 10B and 10C and Table). Additionally, both septal and free wall stress were  $\approx$ 60% lower in HMGB1-treated hearts than in GST-treated hearts (Figure 11A and 11B and Table)

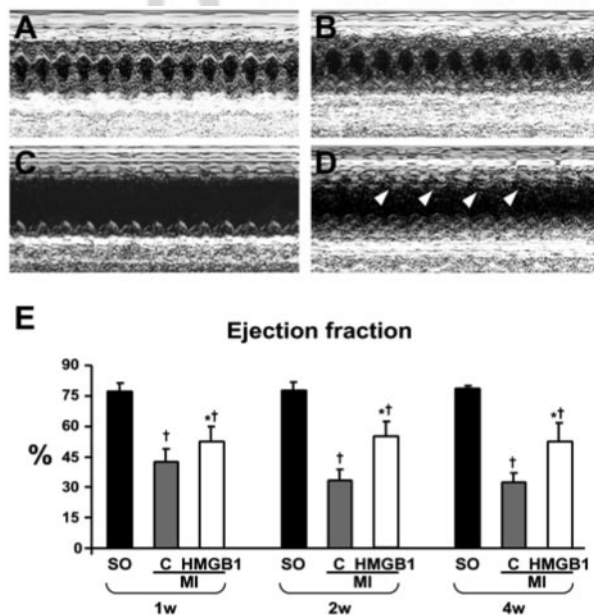


**Figure 9.** Functional assessment of myocardial function by M-mode echocardiography. A through D, Representative M-mode echocardiograms before (A and B) and 1 week after MI (C and D) of mice treated either with GST (C) or HMGB1 (D). Arrowheads indicate contracting cardiac tissue in the area of infarction. Ejection fraction was evaluated at the indicated time points (1, 2, and 4 weeks) in sham-operated (SO) and infarcted mice (MI) treated either with GST (C) or HMGB1. GST-treated mice exhibited a progressive deterioration of the ejection fraction which was prevented in HMGB1-treated mice. \* and †,  $P < 0.001$  at all time points vs C and SO respectively. SO 1 week, n=26; SO 2 weeks, n=16; SO 4 weeks, n=8. C 1 week, n=32; C 2 weeks, n=23; C 4 weeks, n=11. HMGB1 1 week, n=29; HMGB1 2 weeks, n=25; HMGB1 4 weeks, n=13.

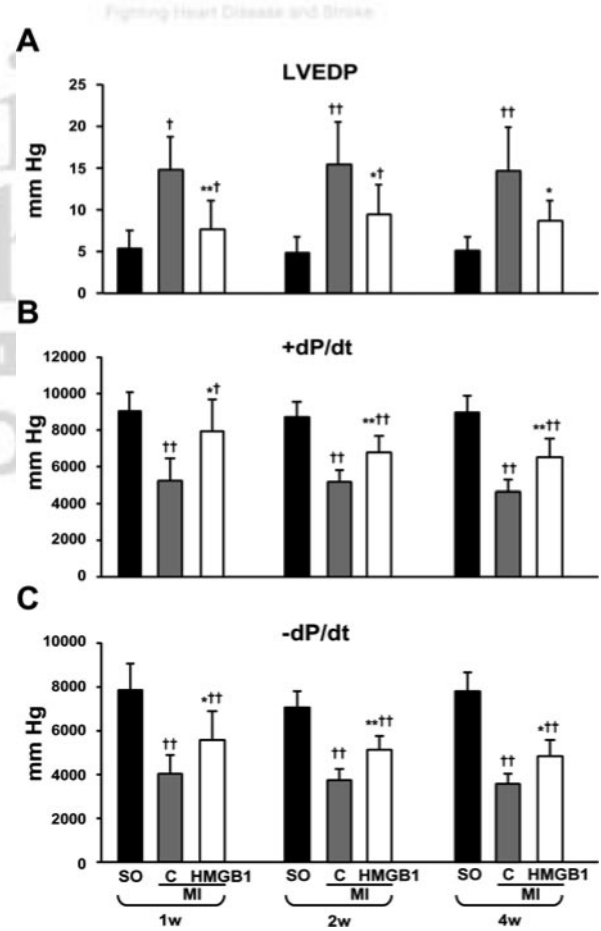


**Figure 10.** Functional assessment of myocardial function, hemodynamic parameters. (A) LVEDP, (B) LV +dP/dt (rate of pressure rise) and (C) LV -dP/dt (rate of pressure decay) in sham-operated (SO) and infarcted mice (MI) treated either with GST (C) or HMGB1. Measurements were obtained 1, 2, and 4 weeks after MI and HMGB1 treatment. \* $P < 0.01$  and \*\* $P < 0.001$  vs C; † $P < 0.01$  and †† $P < 0.001$  vs SO. SO 1 week, n=21; SO 2 weeks, n=8; SO 4 weeks, n=8. C 1 week, n=25; C 2 weeks, n=11; C 4 weeks, n=10. HMGB1 1 week, n=11; HMGB1 2 weeks, n=14; HMGB1 4 weeks, n=9.

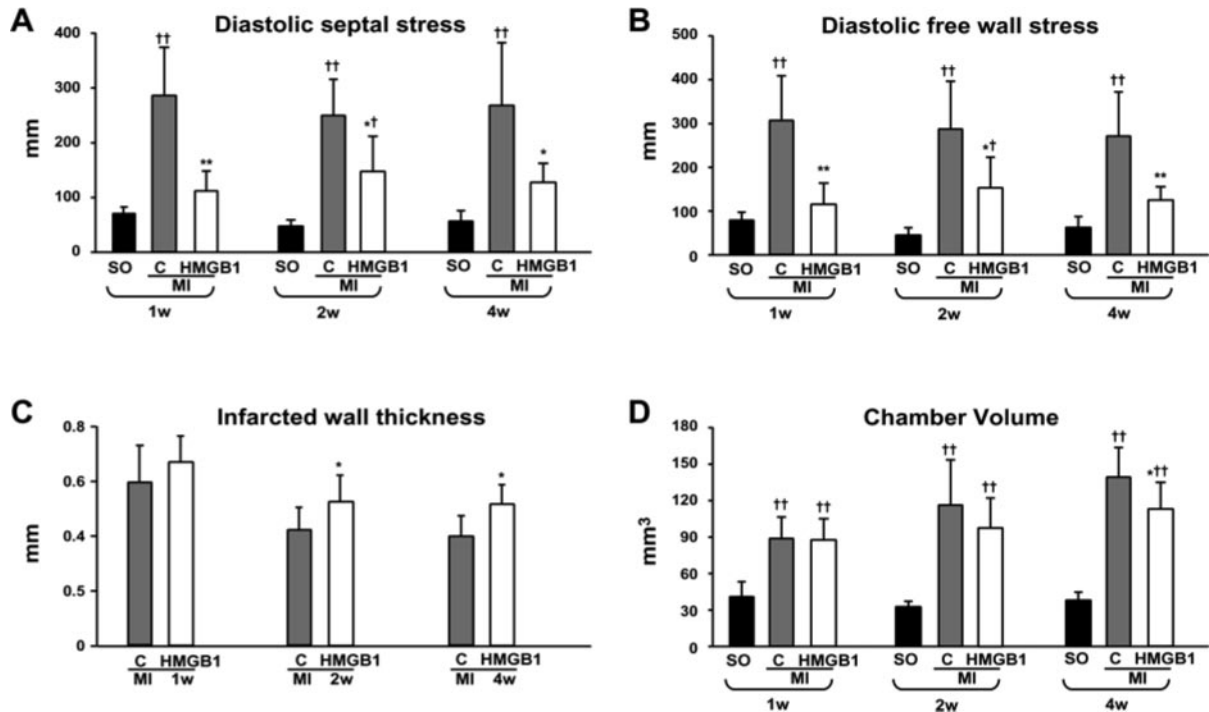


**Figure 11.** Diastolic septal stress (A) and free wall stress (B) in sham-operated (SO) and infarcted mice (MI) treated either with GST (C) or HMGB1. HMGB1-treated hearts exhibited a decrease in the diastolic wall stress at all time points analyzed. C, Infarcted wall thickness was enhanced in HMGB1-treated vs C hearts at 2 and 4 weeks after infarction. D, Left ventricle volume was lower in HMGB1-treated hearts vs C, 4 weeks after infarction. \* $P < 0.01$  and \*\* $P < 0.001$  vs C; † $P < 0.01$ , and †† $P < 0.001$  vs SO. SO 1 week,  $n = 13$ ; SO 2 weeks,  $n = 8$ ; SO 4 weeks,  $n = 8$ . C 1 week,  $n = 26$ ; C 2 weeks,  $n = 9$ ; C 4 weeks,  $n = 14$ . HMGB1 1 week,  $n = 13$ ; HMGB1 2 weeks,  $n = 13$ ; HMGB1 4 weeks,  $n = 11$ .

at all time points. Finally, infarcted wall thickness was significantly enhanced in 2 and 4 weeks HMGB1-treated hearts (Figure 11C and Table), and LV dilation after infarction, as indicated by LV volume, was reduced in HMGB1-treated versus GST-treated hearts (Figure 11D and Table). These results show that myocardial cell regeneration in the infarcted LV wall was associated with a significant improvement in cardiac function and prevented the progression of LV failure and remodeling during the 4 weeks after MI. It is

noteworthy that the improvement of myocardial function after HMGB1 treatment occurred in the presence of a comparable infarct size ( $\approx 53\%$  and  $\approx 54\%$  of the LV of GST- and HMGB1-treated hearts, respectively; data not shown). Functional studies of control mice treated with boxA gave results similar to those obtained with GST (eg, LVEDP at 1 week after coronary artery ligation was  $16 \pm 6.16$  mm Hg in boxA [ $n = 4$ ] versus  $14.84 \pm 3.87$  mm Hg in GST-treated [ $n = 25$ ] control mice).

**Please Provide Title for Table**

	1 Week			2 Weeks			4 Weeks		
	SO	MI	MI+HMGB1	SO	MI	MI+HMGB1	SO	MI	MI+HMGB1
<b>Hemodynamics</b>									
LVEDP, mm Hg	5.4 ± 2.2	14.8 ± 3.9 <sup>a</sup>	7.7 ± 3.4 <sup>ab</sup>	4.9 ± 1.9	15.5 ± 5 <sup>a</sup>	9.4 ± 3.6 <sup>ab</sup>	5.1 ± 1.6	14.8 ± 5.2 <sup>a</sup>	8.7 ± 2.5 <sup>ab</sup>
LV +dP/dt	9043 ± 1067	5263 ± 1222 <sup>a</sup>	7908 ± 1808 <sup>ab</sup>	8775 ± 748	5136 ± 737 <sup>a</sup>	6790 ± 928 <sup>ab</sup>	9012 ± 922	4660 ± 652 <sup>a</sup>	6511 ± 1029 <sup>ab</sup>
LV -dP/dt	7823 ± 1151	4037 ± 803 <sup>a</sup>	5570 ± 1266 <sup>ab</sup>	7028 ± 708	3764 ± 436 <sup>a</sup>	5120 ± 557 <sup>ab</sup>	7737 ± 852	3590 ± 446 <sup>a</sup>	4833 ± 728 <sup>ab</sup>
Diastolic free wall stress	79.2 ± 21.3	309.2 ± 98.1 <sup>a</sup>	123.6 ± 45.5 <sup>b</sup>	49.7 ± 13.6	287.8 ± 107.2 <sup>a</sup>	157 ± 67.5 <sup>ab</sup>	66 ± 23.9	273.3 ± 97 <sup>a</sup>	124.7 ± 34.6 <sup>b</sup>
Diastolic septal stress	72 ± 12.6	284.6 ± 89.2 <sup>a</sup>	113 ± 36.7 <sup>b</sup>	46.1 ± 12.8	248 ± 67.8 <sup>a</sup>	146.5 ± 65.7 <sup>ab</sup>	56.7 ± 19.4	268.5 ± 112 <sup>a</sup>	128.4 ± 33.6 <sup>b</sup>
<b>Echocardiography</b>									
Ejection fraction, %	77.2 ± 4.22	42.7 ± 6.3 <sup>a</sup>	52.34 ± 7.5 <sup>ab</sup>	77.7 ± 3.9	33.5 ± 5.4 <sup>a</sup>	55 ± 6.9 <sup>ab</sup>	78.5 ± 1.6	32.4 ± 4.8 <sup>a</sup>	52.4 ± 9.1 <sup>ab</sup>
<b>Anatomy and Morph</b>									
Chamber Volume	41.2 ± 12	89.7 ± 17.3 <sup>a</sup>	88.2 ± 17.5 <sup>a</sup>	31.7 ± 5.2	117.3 ± 38 <sup>a</sup>	99.6 ± 21.6 <sup>a</sup>	37.9 ± 7	140.9 ± 23.9 <sup>a</sup>	114.5 ± 20.4 <sup>ab</sup>
Infarcted wall thickness		0.6 ± 0.1	0.7 ± 0.08		0.4 ± 0.07	0.5 ± 0.09 <sup>b</sup>		0.4 ± 0.15	0.56 ± 0.12 <sup>b</sup>

Data are presented as mean ± SD.

<sup>a</sup>Statistically significant difference from SO; <sup>b</sup>statistically significant difference from MI.

SO indicates sham-operated; MI+HMGB1, myocardial infarction HMGB1-treated.

The present experiments were not designed to establish the long-term effect of HMGB1 on survival; however, at 35 days after infarction, survival rates between control and HMGB1 groups were comparable at 69% and 65%, respectively.

### Discussion

The present study shows that HMGB1 injection into the mouse heart at the time of MI induced myocardial regeneration and improved cardiac function. Newly formed cardiomyocytes were present in the infarcted area and expressed cardiac markers MEF2C,  $\alpha$ -sarcomeric actin, and connexin 43. In agreement with prior studies of stem cell differentiation into cardiomyocytes, the newly formed cells were rod-shaped but significantly smaller than adult myocardial cells.<sup>30</sup> LV function was evaluated both by echocardiography and hemodynamically in the 4 weeks after coronary artery ligation and was enhanced versus control. Progressive LV dilation occurred in the 4 weeks after MI in control mice, and this event was partially prevented in HMGB1-treated hearts. Cell responses elicited by HMGB1 are mediated, at least in part, by its interaction with the receptor RAGE, which is present on c-kit<sup>+</sup> cardiac cells. The beneficial effects of HMGB1 were associated with cardiac c-kit<sup>+</sup> cell proliferation and differentiation in vivo. Interestingly, c-kit<sup>+</sup> cardiac cell differentiation toward the myocardial lineage was not observed in noninfarcted HMGB1-treated hearts. However, in the presence of acute MI, HMGB1 induced c-kit<sup>+</sup> cells to differentiate into cardiomyocytes, suggesting that signals released from damaged tissue are required for differentiation. Cardiac c-kit cells migrated in vitro in response to HMGB1. In contrast, no evidence of cell motion in response to HMGB1 was found ex vivo by two-photon microscopy. Conversely, both hepatocyte growth factor and insulin growth factor-1 have been previously shown to induce c-kit<sup>+</sup> cell locomotion into the border zone of the infarcted heart.<sup>32</sup> This result needs to be reconciled with the in vitro effect. The possibility that cell migration did occur but could not be detected because of technical limitations of the two-photon microscopy experiment should be considered. This technique detects cell motion up to 200  $\mu$ m from the epicardium. The LV wall thickness in the mouse is  $\approx$ 1 mm. Furthermore, the heart was not beating, and it was perfused with Tyrode solution rather than with blood.

One important issue is whether HMGB1 acted only on c-kit<sup>+</sup> resident cardiac stem cells, which are present in the adult heart,<sup>2-5,33</sup> or also on mobilized stem cells from the bone marrow into the systemic circulation. It has been shown that bone marrow-derived stem cells are mobilized after MI; they can be recruited into the infarcted area,<sup>34-37</sup> and some of these cells express early cardiac markers, such as GATA4 and Nkx2.5.<sup>38,39</sup> However, the magnitude of this phenomenon is so limited that it unlikely has functional significance. In contrast, bone marrow cell mobilization with granulocyte colony-stimulating factor markedly increases circulating stem cell number and leads to myocardial wall regeneration after MI.<sup>26</sup> In the present study, HMGB1 treatment did not induce stem cell mobilization into the systemic circulation. Importantly, tail-vein-injected bone marrow-derived c-kit<sup>+</sup> cells did not significantly participate in HMGB1-mediated cardiac

regeneration. Indeed, newly formed myocytes in the infarcted area were not derived from the peripheral circulation. This finding strongly supports the cardiac origin of c-kit<sup>+</sup> cells involved in HMGB1-mediated myocardial regeneration.

HMGB1 is massively released by necrotic cells as well as by monocytes and macrophages.<sup>14-16</sup> However, under the experimental conditions of the present study, there was no endogenous HMGB1 increase in the heart up to 24 hours after coronary artery ligation, and no increase in CD45<sup>+</sup> cells in response to HMGB1 injection in the infarcted heart was found. Therefore, exogenous HMGB1 injected into the heart in a critical time window, before necrosis occurred, provided the trigger for c-kit<sup>+</sup> cell proliferation and differentiation. It is noteworthy that HMGB1 has been reported to have both beneficial and detrimental effects,<sup>40</sup> and these opposite actions were observed in response to "low" and "high" HMGB1 levels, respectively. HMGB1 actively secreted by inflammatory and other cells plays a key role as a mediator of endotoxic lethality in septic shock in mice.<sup>15</sup> In the present study, 200 ng HMGB1 was administered locally whereas septic-shock induction required the intraperitoneal injection of 500  $\mu$ g HMGB1,<sup>15</sup> a 2500-fold difference which is likely to provide an adequate therapeutic window for the eventual clinical use of this protein.

In summary, the present study shows that exogenous HMGB1 induces resident cardiac c-kit<sup>+</sup> cell proliferation and differentiation in the infarcted heart and provides a novel potential strategy to induce myocardial regeneration, enhance LV function, and partially prevent LV remodeling after coronary artery occlusion.

### Acknowledgments

This research was supported by grant from Italian Ministry of Health and EU FP6 contract number LSHD-CT-2004-5029288 (Application and process optimization of stem cell products for myocardial repair, SC&CR). We thank F. Martelli for the critical reading of the manuscript; R. De Mori, S. Straino, and A. Diamantini for technical support; A. Santini and G. Pennasilico for their assistance with the Echocardiography. We also thank Maurizio Inzillo and the Medical Imaging Service of Istituto Dermopatico dell'Immacolata for figure preparation.

F.L., A.G., M.E.B. and M.C.C. are owners of the patent number WO2004004763 (Use of HMGB1 in the treatment of tissue damage and/or to promote tissue repair). M.E.B. declares further financial interests: he is founder and owner of HMGBiotech; Milano, Italy (a small biotech specializing in HMG proteins), and his laboratory receives funding from the small pharma companies Critical Therapeutics, Inc (Lexington, MA) and Creabilis Therapeutics (Ivrea, Italy) for work related to HMGB1 (although for none of the work reported here). The value of these interests exceeds \$10 000.

### References

1. Wollert KC, Drexler H. Clinical applications of stem cells for the heart. *Circ Res*. 2005;96:151-163.
2. Hierlihy AM, Seale P, Lobe CG, Rudnicki MA, Megney LA. The post-natal heart contains a myocardial stem cell population. *FEBS Lett*. 2002;530:239-243.
3. Nadal-Ginard B, Kajstura J, Leri A, Anversa P. Myocyte death, growth, and regeneration in cardiac hypertrophy and failure. *Circ Res*. 2003;92:139-150.
4. Beltrami AP, Barlucchi L, Torella D, Baker M, Limana F, Chimenti S, Kasahara H, Rota M, Musso E, Urbaneck K, Leri A, Kajstura J, Nadal-Ginard B, Anversa P. Adult cardiac stem cells are multipotent and support myocardial regeneration. *Cell*. 2003;114:763-776.

5. Messina E, De Angelis L, Frati G, Morrone S, Chimenti S, Fiordaliso F, Salio M, Battaglia M, Latronico MV, Coletta M, Vivarelli E, Frati L, Cossu G, Giacomello A. Isolation and expansion of adult cardiac stem cells from human and murine heart. *Circ Res*. 2004;95:911–921.
6. Dawn B, Stein AB, Urbanek K, Rota M, Whang B, Rastaldo R, Torella D, Tang XL, Rezazadeh A, Kajstura J, Leri A, Hunt G, Varma J, Prabhu SD, Anversa P, Bolli R. Cardiac stem cells delivered intravascularly traverse the vessel barrier, regenerate infarcted myocardium, and improve cardiac function. *Proc Natl Acad Sci U S A*. 2005;102:3766–3771.
7. Linke A, Muller P, Nurzynska D, Casarsa C, Torella D, Nascimbene A, Castaldo C, Cascapera S, Bohm M, Quaini F, Urbanek K, Leri A, Hintze TH, Kajstura J, Anversa P. Stem cells in the dog heart are self-renewing, clonogenic, and multipotent and regenerate infarcted myocardium, improving cardiac function. *Proc Natl Acad Sci U S A*. 2005;102:8966–8971.
8. Calogero S, Grassi F, Aguzzi A, Voigtlander T, Ferrier P, Ferrari S, Bianchi ME. The lack of chromosomal protein Hmg1 does not disrupt cell growth but causes lethal hypoglycaemia in newborn mice. *Nat Genet*. 1999;22:276–280.
9. Bustin M. Regulation of DNA-dependent activities by the functional motifs of the high-mobility-group chromosomal proteins. *Mol Cell Biol*. 1999;19:5237–5246.
10. Bustin M, Neihart NK. Antibodies against chromosomal HMG proteins stain the cytoplasm of mammalian cells. *Cell*. 1979;16:181–189.
11. Fages C, Nolo R, Huttunen HJ, Eskelinen E, Rauvala H. Regulation of cell migration by amphoterin. *J Cell Sci*. 2000;113:611–620.
12. Rauvala H, Huttunen HJ, Fages C, Kaksonen M, Kinnunen T, Imai S, Raulo E, Kilpelainen I. Heparin-binding proteins HB-GAM (pleiotrophin) and amphoterin in the regulation of cell motility. *Matrix Biol*. 2000;19:377–387.
13. Taguchi A, Blood DC, del Toro G, Canet A, Lee DC, Qu W, Tanji N, Lu Y, Lalla E, Fu C, Hofmann MA, Kislinger T, Ingram M, Lu A, Tanaka H, Hori O, Ogawa S, Stern DM, Schmidt AM. Blockade of RAGE-amphoterin signalling suppresses tumour growth and metastases. *Nature*. 2000;405:354–360.
14. Wang H, Vishnubhakat JM, Bloom O, Zhang M, Ombrellino M, Sama A, Tracey KJ. Proinflammatory cytokines (tumor necrosis factor and interleukin 1) stimulate release of high mobility group protein-1 by pituitary cells. *Surgery*. 1999;126:389–392.
15. Wang H, Bloom O, Zhang M, Vishnubhakat JM, Ombrellino M, Che J, Frazier A, Yang H, Ivanova S, Borovikova L, Manogue KR, Faist E, Abraham E, Andersson J, Andersson U, Molina PE, Abumrad NN, Sama A, Tracey KJ. HMG-1 as a late mediator of endotoxin lethality in mice. *Science*. 1999;285:248–251.
16. Ombrellino M, Wang H, Ajemian MS, Talhouk A, Scher LA, Friedman SG, Tracey KJ. Increased serum concentrations of high-mobility-group protein 1 in haemorrhagic shock. *Lancet*. 1999;354:1446–1447.
17. Scaffidi P, Misteli T, Bianchi ME. Release of chromatin protein HMGB1 by necrotic cells triggers inflammation. *Nature*. 2002;418:191–195.
18. Fiuza C, Bustin M, Talwar S, Tropea M, Gerstenberger E, Shelhamer JH, Suffredini AF. Inflammation-promoting activity of HMGB1 on human microvascular endothelial cells. *Blood*. 2003;101:2652–2660.
19. Hori O, Brett J, Slattery T, Cao R, Zhang J, Chen JX, Nagashima M, Lundh ER, Vijay S, Nitecki D, et al. The receptor for advanced glycation end products (RAGE) is a cellular binding site for amphoterin. Mediation of neurite outgrowth and coexpression of rage and amphoterin in the developing nervous system. *J Biol Chem*. 1995;270:25752–25761.
20. Parkkinen J, Raulo E, Merenmies J, Nolo R, Kajander EO, Baumann M, Rauvala H. Amphoterin, the 30-kDa protein in a family of HMGB1-type polypeptides. Enhanced expression in transformed cells, leading edge localization, and interactions with plasminogen activation. *J Biol Chem*. 1993;268:19726–19738.
21. Huttunen HJ, Kuja-Panula J, Rauvala H. Receptor for advanced glycation end products (RAGE) signaling induces CREB-dependent chromogranin expression during neuronal differentiation. *J Biol Chem*. 2002;277:38635–38646.
22. Degryse B, Bonaldi T, Scaffidi P, Muller S, Resnati M, Sanvito F, Arrighi G, Bianchi ME. The high mobility group (HMG) boxes of the nuclear protein HMGB1 induce chemotaxis and cytoskeleton reorganization in rat smooth muscle cells. *J Cell Biol*. 2001;152:1197–1206.
23. Palumbo R, Sampaoli M, De Marchis F, Tonlorenzi R, Colombetti S, Mondino A, Cossu G, Bianchi ME. Extracellular HMGB1, a signal of tissue damage, induces mesoangioblast migration and proliferation. *J Cell Biol*. 2004;164:441–449.
24. Muller S, Bianchi ME, Knapp S. Thermodynamics of HMGB1 interaction with duplex DNA. *Biochemistry*. 2001;40:10254–10261.
25. Li Q, Li B, Wang X, Leri A, Jana KP, Liu Y, Kajstura J, Baserga R, Anversa P. Overexpression of insulin-like growth factor-1 in mice protects from myocyte death after infarction, attenuating ventricular dilation, wall stress, and cardiac hypertrophy. *J Clin Invest*. 1997;100:1991–1999.
26. Orlic D, Kajstura J, Chimenti S, Limana F, Jakoniuk I, Quaini F, Nadal-Ginard B, Bodine DM, Leri A, Anversa P. Mobilized bone marrow cells repair the infarcted heart, improving function and survival. *Proc Natl Acad Sci U S A*. 2001;98:10344–10349.
27. Li B, Setoguchi M, Wang X, Andreoli AM, Leri A, Malhotra A, Kajstura J, Anversa P. Insulin-like growth factor-1 attenuates the detrimental impact of nonocclusive coronary artery constriction on the heart. *Circ Res*. 1999;84:1007–1019.
28. Orlic D, Kajstura J, Chimenti S, Jakoniuk I, Anderson SM, Li B, Pickel J, McKay R, Nadal-Ginard B, Bodine DM, Leri A, Anversa P. Bone marrow cells regenerate infarcted myocardium. *Nature*. 2001;410:701–705.
29. Guerra S, Leri A, Wang X, Finato N, Di Loreto C, Beltrami CA, Kajstura J, Anversa P. Myocyte death in the failing human heart is gender dependent. *Circ Res*. 1999;85:856–866.
30. Limana F, Urbanek K, Chimenti S, Quaini F, Leri A, Kajstura J, Nadal-Ginard B, Izumo S, Anversa P. bcl-2 overexpression promotes myocyte proliferation. *Proc Natl Acad Sci U S A*. 2002;99:6257–6262.
31. Anversa P, Nadal-Ginard B. Myocyte renewal and ventricular remodelling. *Nature*. 2002;415:240–243.
32. Rastaldo R, Baker M, S C, Rota M, Torella D, Muller P, Musso E, Sonnenblick EH, Nadal-Ginard B, Urbanek K, Leri A, P A. Translocation of Cardiac Primitive Cells to the Infarcted Myocardium Occurs through the Interstitial Compartment, Independently from the Coronary Circulation. In: *Circulation*, American Heart Association; 2003.
33. Laugwitz KL, Moretti A, Lam J, Gruber P, Chen Y, Woodard S, Lin LZ, Cai CL, Lu MM, Reth M, Platoshyn O, Yuan JX, Evans S, Chien KR. Postnatal is11+ cardioblasts enter fully differentiated cardiomyocyte lineages. *Nature*. 2005;433:647–653.
34. Asahara T, Masuda H, Takahashi T, Kalka C, Pastore C, Silver M, Kearne M, Mager M, Isner JM. Bone marrow origin of endothelial progenitor cells responsible for postnatal vasculogenesis in physiological and pathological neovascularization. *Circ Res*. 1999;85:221–228.
35. Jackson KA, Majka SM, Wang H, Pocius J, Hartley CJ, Majesky MW, Entman ML, Michael LH, Hirschi KK, Goodell MA. Regeneration of ischemic cardiac muscle and vascular endothelium by adult stem cells. *J Clin Invest*. 2001;107:1395–1402.
36. Shintani S, Murohara T, Ikeda H, Ueno T, Honma T, Katoh A, Sasaki K, Shimada T, Oike Y, Imaizumi T. Mobilization of endothelial progenitor cells in patients with acute myocardial infarction. *Circulation*. 2001;103:2776–2779.
37. Goodell MA, Brose K, Paradis G, Conner AS, Mulligan RC. Isolation and functional properties of murine hematopoietic stem cells that are replicating *in vivo*. *J Exp Med*. 1996;183:1797–1806.
38. Kucia M, Dawn B, Hunt G, Guo Y, Wyszczynski M, Majka M, Ratajczak J, Rezzoug F, Ildstad ST, Bolli R, Ratajczak MZ. Cells expressing early cardiac markers reside in the bone marrow and are mobilized into the peripheral blood after myocardial infarction. *Circ Res*. 2004;95:1191–1199.
39. Wojakowski W, Tendera M, Michalowska A, Majka M, Kucia M, Maslankiewicz K, Wyderka R, Ochala A, Ratajczak MZ. Mobilization of CD34/CXCR4+, CD34/CD117+, c-met+ stem cells, and mononuclear cells expressing early cardiac, muscle, and endothelial markers into peripheral blood in patients with acute myocardial infarction. *Circulation*. 2004;110:3213–3220.
40. Lotze MT, Tracey KJ. High-mobility group box 1 protein (HMGB1): nuclear weapon in the immune arsenal. *Nat Rev Immunol*. 2005;5:331–342.